Mizoroki-Heck Macrocyclization Reactions at 1 M Concentration Catalyzed by Sub-nanometric Palladium Clusters

Francisco Garnes-Portolés,[a] Estíbaliz Merino,[b, c] and Antonio Leyva-Pérez*[a]

The synthesis of cyclized organic compounds with more than ten atoms (macrocycles) is traditionally based on reversible reactions under highly diluted conditions, typically < 0.05 M, in order to circumvent the formation of intermolecular products. These reaction conditions severely hamper industrial productivity and the use of solid catalysts. Herein, it is shown that the intramolecular Mizoroki-Heck reaction of ω-iodide cinnamates proceeds at 1 M concentration when catalyzed by few-atom Pd clusters, either in solution or supported on a solid, to give different macrocycles in good yields. This paradigmatic increase in reaction concentration not only opens the door for macrocycle production with high throughputs but also enables the use of solid catalysts for a macrocyclization reaction in flow.

Introduction

Macrocyclic molecules (macrocycles) are organic cycles with more than ten atoms, which are abundantly distributed in nature and have an enormous impact on the fields of chemistry, biology, and medicine.[1,2] Historically, macrocycles have been obtained from natural sources to provide unique drugs such as rapamycin, erythromycin, epothilone, vancomycin, and cyclosporine, to name a few (Figure S1 in the Supporting Information).[3] As far as we know, big volume synthetic macrocycle feedstocks are very scarce and only cyclododecatriene and cyclododecanone are employed as starting materials in the manufacturing of some fragrances (Figure S2). The unsustainability of plant/animal destruction to obtain a limited amount of any macrocycle, together with the retrosynthetic limitations imposed by the C_{12} symmetry of cyclododecatriene/cyclododecanone and the need of new macrocycles for drug discovery, has spurred the exploration of different synthetic strategies to

achieve macrocycles, particularly in the last years.[4] However, the macrocyclization reaction is still the bottleneck in any macrocycle synthetic strategy, in terms of price, efficiency and waste-generation, and mostly determines the overall effectiveness of the synthetic route.[5]

Figure 1 shows that, in order to circumvent the entropic penalty associated to the intramolecular reaction and avoid the corresponding intermolecular reactions, particularly those forming irreversible single carbon—carbon bonds instead of reversible unsaturated carbon—carbon bonds (i.e. alkene[6] and alkyne[7] metathesis) or carbon—heteroatom bonds (macrolactonization and macrolactamization), the most protocols reported so far involve high dilution conditions.[8] Reaction concentration is crucial for product outcome, thus it is not surprising that most of the reported macrocyclization procedure highlight the value for concentration, particularly when this value is ~ 10 mM, which is called "moderate dilution conditions".[9] A simple calculation gives that, even for the smallest of the macrocycles that could be considered (molecular weight ~ 200 Da.), a 500:1 solvent-to-substrate ratio (500 kg or L of solvent per kg of

[a] F. Garnes-Portolés, Dr. A. Leyva-Pérez
     Instituto de Tecnología Química (UPV-CSIC)
     Universidad Politècnica de València Consejo Superior de
     Investigaciones Científicas
     Avda. de los Naranjos s/n, 46022 Valencia (Spain)
     E-mail: anleyva@itq.upv.es
[b] Dr. E. Merino
     Universidad de Alcalá,
     Departamento de Química Orgánica y Química Inorgánica,
     Instituto de Investigación Química "Andrés M. del Río" (IQAR)
     Facultad de Farmacia,
     Alcalá de Henares, 28805 Madrid (Spain)
[c] Dr. E. Merino
     Instituto Ramón y Cajal de Investigación Sanitaria (IRYCIS)
     Ctra. de Colmenar Viejo, Km. 9.100, 28034, Madrid (Spain)
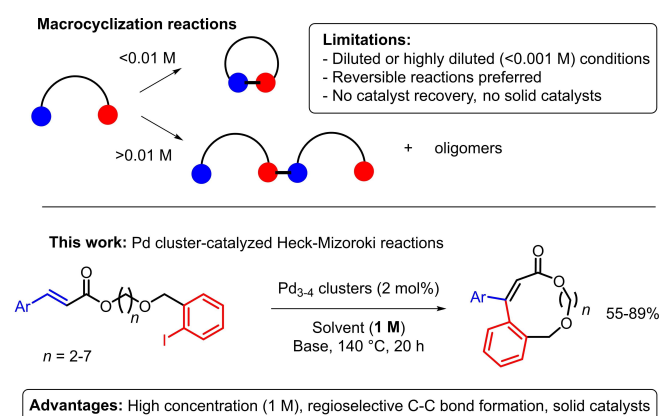
Figure 1. Non-diluted Mizoroki-Heck macrocyclization reactions.

macrocycle) is required under these "moderate dilution con-ditions". Much worse, macrocyclization reactions are routinely performed at higher dilutions, 1 mM ("high dilution") or < 1 mM conditions ("very high dilution conditions").[10] It is obvious that these reactions are unpractical and highly inefficient not only in the laboratory but also in an industrial environment, where throughput is money and long reaction times and large amounts of solvent are unacceptable, not only from an economic point of view but also from the prospects of green chemistry and sustainability.[11]

Solid catalysts are preferred in industry because of their easier handling and recovery, and the possibility of in-flow processes. For the successful implementation of a solid catalyst in a given liquid-phase reaction, a certain dilution threshold has to be overcome, otherwise the inherent diffusion limitations imparted by the solid together with the high dilution, makes the solid-catalyzed system unacceptably low active. This is the reason why, to our knowledge, solid-catalyzed macrocyclization reactions have not been reported yet, despite the need of improving the throughput for these reactions was early recognized, and solid-phase reagents were employed.[12] There-fore, the discovery of a highly concentrated macrocyclization reaction will incidentally enable the use of solid catalysts and the design of catalytic macrocyclization reactions in flow.
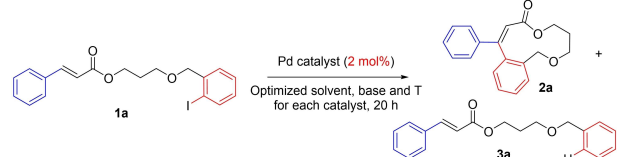
Here we show a carbon–carbon bond-forming macrocycli-zation reaction which operates at 1 M concentration (5 : 1 solvent-to-substrate ratio) and employs, if desired, solid cata-lysts. Figure 1 shows the synthetic strategy, which is based on a Pd cluster-catalyzed Mizoroki-Heck reaction. Pd clusters catalyze well the intramolecular but not the intermolecular Mizoroki-Heck reaction of 1,2-disubstituted alkenes[13a,b,14] thus, in principle, the macrocyclization reaction between the ω-halide and the internal alkene functional groups of the linear molecule will occur without the necessity of dilution, since no intermo-lecular reactions compete. Despite different Pd-catalyzed cross-coupling reactions have been previously reported for macro-cyclization reactions, all of them use concentrations between < 0.001 and 0.22 M (in exceptional cases), including the Mizoroki-Heck,[15] Stille,[16] Suzuki–Miyaura,[17] Sonogashira,[18] Tsuji-Trost,[19] and C—H activation reactions.[20] In all these examples, the intermolecular couplings still occur with the Pd catalyst and under the reaction conditions employed. In contrast, the ligand-free Pd$_{3-4}$ cluster here reported facilitates the selective intramolecular coupling between the C—I and C=C bonds of the macrocycle, after coordination to different Pd atoms of the cluster, without the entropic and steric penalties associated to closed-shell monoatomic Pd complexes. In this way, the macrocyclization Mizoroki-Heck reaction occurs effi-ciently at high concentrations and enables the use of solid-supported Pd$_{3-4}$ clusters as recoverable catalysts for the reaction.

Results and Discussion

Discovery of the Mizoroki-Heck macrocyclization reaction at 1 M concentration and optimization of the reaction conditions

The linear ω-iodide cinnamate **1a** was prepared by esterifica-tion of cinnamic acid with 1,3-propanediol and later benzylation with o-iodobenzyl bromide (see Supporting Information for the synthesis of substrates). Isolated **1a** was then tested in the intramolecular Mizoroki-Heck reaction with different typical Pd catalysts, under the optimized reaction conditions for each catalyst.[21] Table 1 shows that none of the Pd complexes tested catalyzed, in our hands, the macrocyclization reaction of **1a** at 0.1 M concentration (entries 1–6), but just the dehydrohaloge-nation reaction to give product **3a**. In contrast, Pd$_{3-4}$ clusters gave macrocycle **2a** in 76% yield (entry 7). It is worth commenting here that the Pd complexes tested in entries 1–6 were also ineffective under the reaction conditions in entry 7, provided that Pd$_{3-4}$ clusters are not formed. Remarkably, the good yield for **2a** was kept after increasing the reaction concentration from 0.2 M to 1 M (entries 8–10), to get a 66% yield of **2a** at 1 M concentration. This result corresponds to a macrocyclization efficiency index (E_{mac}, defined as $\log_{10}$[yield (%)^3 concentration (mmol L^{-1})]) = 8.46, among the highest in the literature.[22] The Pd$_{3-4}$ cluster catalyst can be either formed in-situ or prepared independently and added to the reaction.[13a,b,14a] The dimerization of **1a** was not observed according to gas-chromatography mass-spectrometry (GC-MS) and ^{1}H and ^{13}C nuclear magnetic resonance (NMR) spectro-scopy, and also to distortionless enhancement by polarization transfer (DEPT) measurements. The only by-product found was,

Table 1. Macrocyclization Mizoroki-Heck reaction of linear ω-iodide cinna-mate **1a** to macrocycle **2a** catalyzed by different Pd complexes and Pd$_{3-4}$ clusters.[a]

Entry	Pd catalyst	Reaction conditions	[mol L^{-1}]	Yield[b] [%] 2a	3a
1	Pd(OAc)$_2$	Cy$_2$NMe,[c]	0.1	–	10
2	Pd(PPh$_3$)$_4$	toluene,		2	70
3	PdCl$_2$(PPh$_3$)$_2$	100 °C		6	83
4	Pd(OAc)$_2$, SPhos			–	20
5	Nájera's Catalyst			10	90
6	PEPPSI-^{i}Pr-Pd[d]			3	80
7	Pd$_{3-4}$	Na$_2$CO$_3$	0.1	76	24
8		(2 equiv.),	0.2	84	16
9		NMP,[e]	0.5	69	31
10		140 °C	1	66	34

[a] The structure of the Pd complexes are shown in Figure S3, mass balances are > 99% in all cases; see Table S1 for reaction optimization with Pd$_{3-4}$ clusters. [b] Isolated yields. [c] Cy$_2$NMe: dicyclohexylmeth-ylamine. [d] PEPPSI-^{i}Pr—Pd: [1,3-bis(2,6-diisopropylphenyl)imidazol-2-ylidene](3-chloropyridyl)palladium(II) dichloride. [e] NMP: N-methyl pyrroli-done.

ChemSusChem

Research Article
doi.org/10.1002/cssc.202300200

**Chemistry
Europe**
European Chemical
Societies Publishing

again, dehalogenated cinnamate **3a**, and mass balances were >99% in all cases. The best yields of **2a** were obtained with *N*-methyl pyrrolidone (NMP) as a solvent and Na$_2$CO$_3$ as a base, however, other bases and solvents can also be employed (Table S1). In particular, the use of *N,N*-diisopropylamine (DIPEA) as a base enabled a one-pot procedure (see ahead).

With the above results in hand, different macrocyclization reactions catalyzed by in-situ formed Pd$_{3-4}$ clusters were carried out. Some nanoparticles can be formed together with the ultrasmall clusters, however, the former does not catalyze the Mizoroki-Heck reaction under these reaction conditions.[13a] Figure 2 shows that different macrocycles with eleven (**2a–c**) and fifteen atom membered rings (**2d–e**) could be synthesized from the corresponding linear substrates **1a–e** in moderate to good yields at reaction concentrations between 0.1 M and 1 M, without significant yield decrease when increasing the reaction concentration. An $E_{mac} = 8.69$ is obtained for **2d** at 1 M concentration, which is, to our knowledge, the highest reported to date.[22a] The corresponding dehalogenated by-products **3a–e** complete the mass balance. Nitro and methoxy substituents are tolerated during reaction, and other different functional groups are expected to be also tolerated under these typical Jeffery-type reaction conditions.[23]
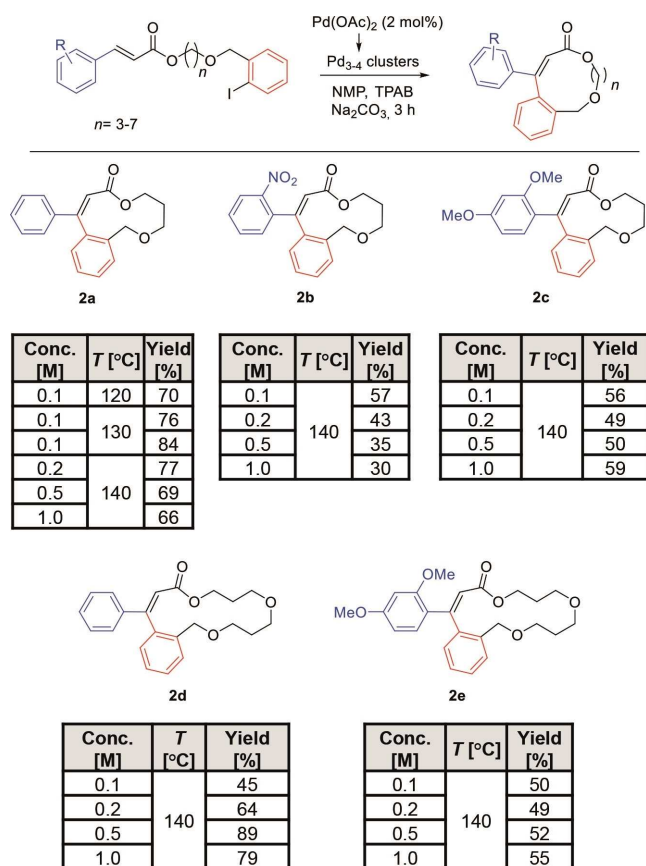
Expanding the scope with one-pot reactions

In order to avoid the synthesis and isolation of the precursors **1a–e**, the macrocyclization reaction was performed in one-pot from the corresponding cinnamate precursors, and the results are shown in Figure 3. It can be seen that the incorporation of the iodide moiety to the cinnamate part occurs without any solvent in the presence of DIPEA as a base, to give intermediates **1a–i**. Then, the Pd precursor, tetrapropylammonium bromide (TPAB) and NMP are added to the solution to generate the Pd$_{3-4}$ clusters, and the reaction is run in the same reaction conditions as with the isolated linear cinnamates **1a–e**, to give macrocycles **2a–i** in reasonable isolated yields. These yields are in most cases better compared to the two steps procedure (compare Figures 2 and 3). For instance, product **2b** increases from 30% in the two steps procedure to 55% yield in the one-step procedure. It is true that the substrate scope here shown is narrow and, for instance, if the aryl group is not present in the alkene, the reaction does not proceed, however, this intramolecular Mizoroki-Heck coupling is, to our knowledge, an unique example of macrocyclization reaction at 1 M concentration.
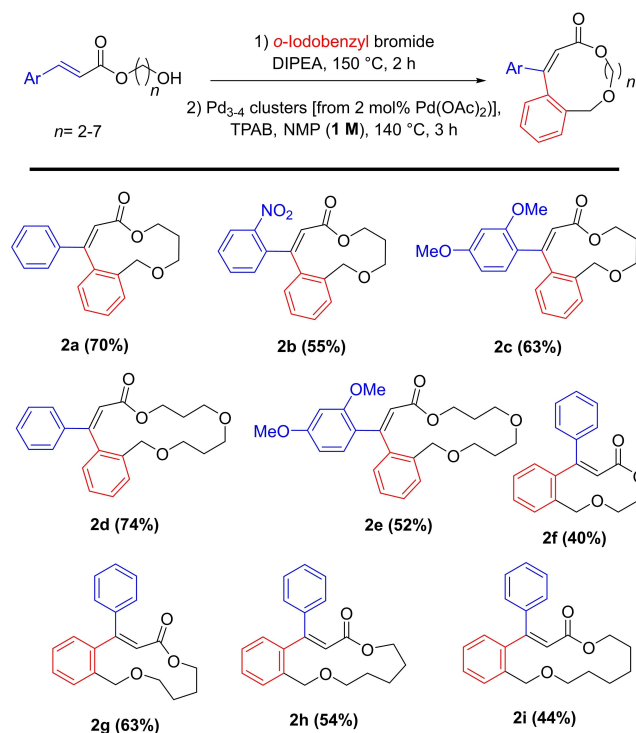

Conc. [M]	T [°C]	Yield [%]
0.1	120	70
0.1	130	76
0.1		84
0.2		77
0.5	140	69
1.0		66

Conc. [M]	T [°C]	Yield [%]
0.1		57
0.2	140	43
0.5		35
1.0		30

Conc. [M]	T [°C]	Yield [%]
0.1		56
0.2	140	49
0.5		50
1.0		59

Conc. [M]	T [°C]	Yield [%]
0.1		45
0.2	140	64
0.5		89
1.0		79

Conc. [M]	T [°C]	Yield [%]
0.1		50
0.2	140	49
0.5		52
1.0		55

Figure 2. Synthesis of macrocycles **2a–e** with Pd$_{3-4}$ clusters at 0.1–1 M reaction concentrations. GC yields.

Figure 3. One-pot synthesis of macrocycles **2a–i** with Pd$_{3-4}$ cluster catalyst at 1 M reaction concentrations. Isolated yields.

ChemSusChem

Research Article
doi.org/10.1002/cssc.202300200

**Chemistry
Europe**
European Chemical
Societies Publishing

Reaction mechanism

Dehalogenation by-reaction

The origin of the dehalogenated compound **3a** was then studied. The use of isotopically enriched *N,N*-dimethyldeuteroformamide (*d*-DMF, Figure S4) did not give any deuterated product *d*[1]-**3a**, which discards the transfer of H atoms from the solvent to the arene under the Pd-catalyzed reaction conditions. In contrast, the use of thoroughly dried solvents and Na_2CO_3 lowered the amount of **3a** after reaction, which strongly supports a hydrodepalladation reaction as the origin of the dehalogenated compound **3a** (Figure S5).[24] Please notice that the presence of H_2O is beneficial for the stabilization of Pd_{3-4} clusters,[13] thus it is very possible that by-product **3a** comes from hydrated Pd_{3-4} species. To confirm this, kinetic experiments were carried out in the presence or not of TPAB, and the results show that both the macrocyclization and dehalogenated products **2** and **3** are formed by the catalytic action of the TPAB-stabilized Pd clusters and not from neither monoatomic Pd species nor nanoparticles (Figure S6). Indeed, the addition of D_2O to the reaction triggered the formation of deuterated compound *d*[1]-**3a** (Figure S7). These results strongly support that the dehalogenated product **3a** comes from a parasite Pd_{3-4}-catalyzed dehydrohalogenation reaction, which nevertheless can be decreased to a reasonable low extent by excluding water from the reaction mixture.

Alkene insertion as a key step during reaction and role of the oxygen atoms

The rate equation for the macrocyclization of isolated **1a** was obtained on the basis of the initial rates calculated by kinetic experiments at different reagent and catalyst concentrations, and the result showed that the initial reaction rate follows the equation $r_{o,2a} = k_{exp} \cdot [Pd]^1 \cdot [1a]^1 \cdot [Na_2CO_3]^0$ (variables correspond to an experimental constant and the concentration of catalyst and reactants, respectively), thus linearly dependent on the Pd and reactant amounts but independent of the base concentration. This rate equation is in good agreement with previous mechanistic studies for this catalytic system where the rate-determining step of the Mizoroki-Heck reaction is alkene insertion.[12] If this is so, base quenching and Pd re-oxidation will not have any influence in the reaction rate since these chemical events occur after alkene insertion, at later stages during reaction. To confirm this mechanistic hypothesis, two new experiments were performed. First, an O_2 balloon was fit to the reaction mixture, and O_2 did not produce any change in the reaction outcome. Second, the comparatively electron-richer alkene 7-tetradedene was added to the reaction mixture, which completely stopped the Mizoroki-Heck coupling (Figure S8). These results indicate that a potential late re-oxidation of Pd in the catalytic cycle does not change the reaction rate but, in contrast, the addition of an external alkene blocks the Pd_{3-4} clusters action, thus the alkene insertion step is critical in the reaction rate. To further confirm that the alkene insertion and

not the oxidative addition step is rate-determining for the reaction, the rate equation for the dehalogenated product **3a** was also calculated (on the same basis than above), to give $r_{o,3a} = k'_{exp} \cdot [Pd]^1 \cdot [1a]^0 \cdot [Na_2CO_3]^0$. This equation rate shows that the cross-coupling between isolated **1a** and H_2O are not dependent in **1a** but only in the Pd amount. In other words, if the oxidative addition of **1a** on the Pd_{3-4} clusters is not controlling the coupling with H_2O and we assume that this oxidative addition is similar for the Mizoroki-Heck reaction, we may conclude that the alkene insertion step is controlling the latter. Besides, the reaction rate varies significantly when changing the electronics of the cinnamate ring, thus further supporting alkene insertion as the determining step of the catalytic cycle (Table S2).

The activation energy calculated for the macrocyclization reaction with an Arrhenius plot, of either isolated **1a** or **1d**, is similar (~ 36 kcal mol^{-1}), but much higher that when a six-membered ring is formed (compound **1f**, 5.0 kcal mol^{-1}, see Figure S9).[14] These activation energy values keep similar for the formation of the corresponding dehalogenated products **3a** and **3d** (~ 38 kcal mol^{-1}, Figure S9). Thus, these results are consistent with the similar yields found for different chain lengths and with the fact that the dehalogenation reaction easily competes with the Mizoroki-Heck coupling.

The role of oxygen-coordinating atoms for the Pd catalyst was then examined. Methyl cinnamate does not react with *o*-iodobenzyl methyl ether under the optimized Mizoroki-Heck reaction conditions, but indeed does with *p*-iodobenzyl methyl ether, to give the corresponding *p*-Mizoroki-Heck intermolecular coupling product in high yields (Figure S10). The fact that the intermolecular Mizoroki-Heck coupling only proceeds when the carbon atom (C–I) is away (*para* position) from the ether moiety, strongly indicates that the presence of coordinating oxygen atoms in the starting materials **1a**–**l** somehow assists to stop the intermolecular coupling, thus triggering the selective macrocyclization reaction. Notice that the oxidative addition of the C–I bond to the Pd clusters occurs in both cases, since the *o*-substituted reactant gives the homocoupling and dehalogenated products in high yields. The coordinating oxygen atoms are not only those on the ether substituents but can also be those on the cinnamate ester, which is indicated by the slight decrease in yield when increasing the alkyl chain from **2g** to **2i**.

Computational studies

A detailed computational analysis by density functional theory (DFT) calculations was then performed to gain insight into the alkene insertion step, as key of the reaction. The transition states of **1a** with Pd_3 and Pd_4 clusters show that the coordination of the Pd atoms to the sp^2 oxygen atom of the ester group gives the more stable configuration when the atom of iodine is present (**1a**–**Pd₃I**), as shown in Figure 4 (see Figure S11 for the corresponding energy profiles). This **1a**–**Pd₃I** species is favored vs the Pd_4 cluster (**1a**–**Pd₄I**) by $\Delta\Delta G^{\neq} = +5.8$ kcal mol^{-1} (change of Gibbs free energy in the transion state) and vs the corresponding de-iodinated species (**1a**–**Pd₃**
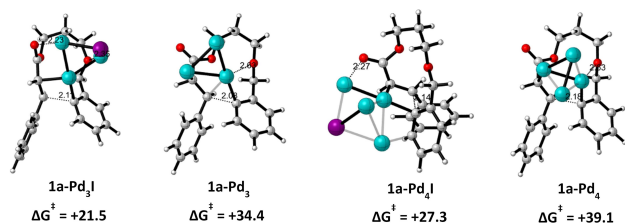
ChemSusChem

Research Article
doi.org/10.1002/cssc.202300200

Chemistry Europe
European Chemical
Societies Publishing

Figure 4. Transition states and energy values (in kcal mol^{-1}) for Pd$_{3-4}$ and Pd$_{3-4}$-I clusters. Geometry optimizations and calculations of electronic energies were performed using: B3LYP/6-311+G(d,p), LANL2DZ for Pd level (gas phase) at 413.15 K. Color code: Pd (blue), I (magenta), O (red), C (grey) and H (white).

and **1a–Pd$_4$**) by $\Delta\Delta G^{\ddagger} = +4.7$ kcal mol^{-1}. For the latter, ether-rather than ester-linked structures are formed, in such a way that the most stable coordination modes of **1a** with Pd$_3$ and Pd$_4$ clusters, without iodine, involve the sp^3 oxygen of the ether group and the C=C bond. Other different potential transition states for Pd$_3$ and Pd$_4$ clusters, with and without the iodine atom, were computed (Figures S12, S13), with higher energies in all cases. For example, the stabilization of transition states by π-stacking (Figure S14) or *ipso*-substitution with the aromatic rings of **1a** (Figure S15) showed $\Delta\Delta G^{\ddagger} \approx +27$–39 and +72 kcal mol^{-1}, respectively.

The difference in the preferred coordinating mode can be explained by the fluxionality of the Pd$_{3-4}$ clusters when joint to the iodine atom. The optimized length of the C–C bond being formed during alkene insertion is similar for Pd$_3$ and Pd$_4$ clusters, ~2.1 Å in both cases, but the different number of additional interactions that can be found between the Pd cluster, the iodine atom and **1a** leads to different values of activation energies. **1a–Pd$_3$I** shows an additional interaction of the Pd atom with the ether group which is not present in **1a–Pd$_4$I**, however, both intermediates could be catalytically productive. Indeed, the experimental activation energy result (~ +37 kcal mol^{-1}, see Figure S9) must be an average of the different catalytically active Pd species in solution (mainly Pd$_{3-4}$ and perhaps other Pd clusters with higher atomicity), thus the experimental and computational values approach, within the margin error of the computed values. Besides, for both Pd$_3$ and Pd$_4$ clusters, two different Pd atoms interact with C$_{sp2}$ atoms in the more favorable transition states. In this way, the intra-molecular reaction is favored over the intermolecular reaction on the **Pd$_3$I** cluster with an energy difference of 13.2 kcal mol^{-1} (Figure S16), which explains why the intramolecular reaction occurs preferentially on the 1 M concentrated medium.

Since the iodine atom can be removed from the cluster before or after the beta-H elimination step, both hypotheses were considered. The energy profile calculated for the **Pd$_3$I** cluster where the removal of the iodine atom occurs first to the formation of the C–C bond (Figure S17, left), is disfavored respect to a transition state that keeps the iodine coordinated with Pd$_3$ (+34.5 vs. 21.5 kcal mol^{-1}, respectively). The same calculations were then performed for the **Pd$_4$I** cluster (Figure S18, right) and the results were similar, with a higher energy associated to the cluster that first dissociated the iodine atom

(+39.1 vs 27.3 kcal mol^{-1}, respectively). In order to discard that single Pd atoms (Pd$_1$), formed in-situ during reaction, could act as potential catalysts, and also to further understand the relative energies associated to a variety of Pd species of different atomicity, the energy associated to the more favorable transition state during alkene insertion based on Pd$_1$ species was computed. The high energy of the **1a–Pd$_1$** transition state (+44.5 kcal mol^{-1}, Figure S18) supports the assumption that a fluxional group is necessary for the alkene insertion reaction to occur.

These results, together, support that iodinated Pd$_{3-4}$ clusters are responsible for the first C–C bond-forming reaction.[25]

Proposed mechanism

With all the above data in hand, Figure 5 shows our proposed mechanism for the macrocyclization Mizoroki-Heck reaction catalyzed by Pd$_{3-4}$ clusters, in this case for the transformation of **1a** to **2a** as a representative example. The mechanism follows the canonical steps of any Mizoroki-Heck reaction, i.e. oxidative addition, alkene migratory insertion and reductive elimination. However, in contrast to other type of Pd catalysts, the multiple coordination of oxygen atoms to the Pd cluster and the flexibility of the latter to concomitantly bear the reacting chemical entities (iodide, alkene and H) on different Pd atoms, is key for the successful cyclization at high concentration. The rate-determining step is the intramolecular alkene migratory insertion. In this way, undesired intermolecular reactions are avoided. This mechanism is supported by kinetic, energetic, reactive, isotopic and computational data.
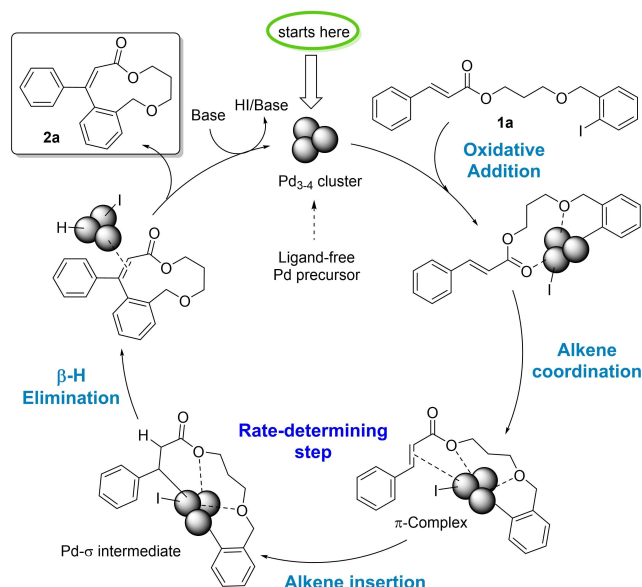

Figure 5. Proposed mechanism for the Pd$_{3-4}$ cluster–catalyzed synthesis macrocycle **2a** at 1 M concentration.

ChemSusChem

Research Article
doi.org/10.1002/cssc.202300200

**Chemistry
Europe**

European Chemical
Societies Publishing

Solid catalysts and macrocyclization in flow

A 1 M concentration reaction is suitable for employing solid instead of soluble catalysts, since diffusion limitations do not significantly control the reaction at this concentration. Thus, the use of supported Pd clusters was evaluated. The solid catalysts were prepared by the iodine disaggregation method previously reported by us and others,[26] to obtain very small Pd clusters on different supports. Table 2 shows the results. Low polar solvents (alkanes and aromatics) were tested since more polar solvents lead to metal leaching. It can be seen that the best results were obtained with Pd on charcoal (Pd$_{3\text{-}4}$/C) catalyst and o-xylene as a solvent (entry 6), to give a 40% yield of **2a**, with nearly the rest (55%) being dehalogenated product **3a**. The latter is the major product in all the conditions tested, even with thoroughly dried solvents, since reactive water must remain on the different supports. Notice that, in homogeneous solution, water can be easily removed by completely drying the solvent, however, the solid catalyst cannot be dried so extensively since the supported Pd clusters would agglomerate. Pd nanoparticles (NPs) gave <6% of product **2a** (entries 11 and 12) under optimized reaction conditions, at 1 M concentration.

A hot filtration test confirmed that Pd$_{3\text{-}4}$/C acts as a truly heterogeneous catalyst and that active Pd species are not present in solution (Figure S19). With these results in hand, we tested Pd$_{3\text{-}4}$/C as a solid catalyst for the macrocyclization Mizoroki-Heck reaction in flow. The reaction was performed in a fixed-bed reactor containing the Pd$_{3\text{-}4}$/C catalyst under a continuous flow of reaction mixture. Figure 6 shows that a 40% yield of product **2a** is formed after 30 min reaction time, and then the yield increases to 55%. However, we were not able to increase the yield of **2a** above 55%, and the yield decreased back to 40% after 50 h on stream.

Nevertheless, this result must be remarked since, to our knowledge, this is the first example of solid-catalyzed macrocyclization reaction in flow.

Table 2. Solid catalyst, solvent and temperature screening for the macrocyclization Mizoroki-Heck reaction of linear ω-iodide cinnamate **1a** to macrocycle **2a**.[a]

Entry	Catalyst	I source	Pd[b]	Solvent	T [°C]	Yield [%]	
						2a	**3a**
1	**Pd$_{3\text{-}4}$/C**	I$_2$	3.5	n-hexane	60	0	0
2				dodecane	130	3	7
3				toluene	100	5	10
4				mesitylene	100	10	30
5					150	15	40
6				**o-xylene**	**100**	**40**	**55**
7					130	10	90
8		EtI	3.8		100	16	50
9	Pd$_{3\text{-}4}$/Al$_2$O$_3$	I$_2$	0.8			1	10
10		EtI	0.9			3	16
11	Pd NPs/C	–	5.0			6	76
12	Pd NPs/Al$_2$O$_3$	–	1.0			2	10

[a] Reaction conditions: Pd (20 mol%), solvent (1 M), Cy$_2$NMe (1.5 equivalents) as a base, 24 h reaction time. [b] wt% in the solid, measured by ICP-AES after disaggregation of the solid in aqua regia and filtration.
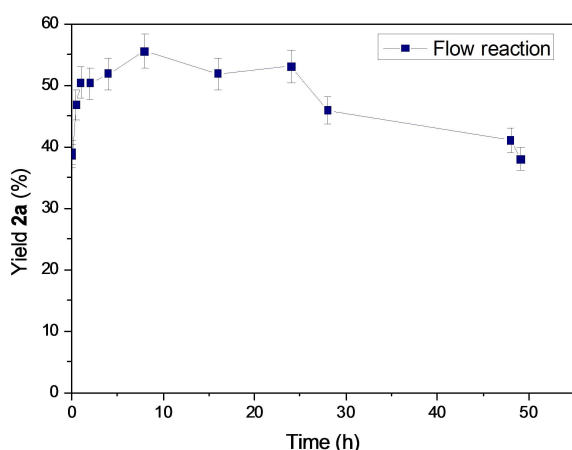
Conclusions

Few atom Pd clusters catalyze the macrocyclization Mizoroki-Heck reaction at 1 M concentration in good yields. Solid Pd catalysts can also be used for this robust macrocyclization reaction based on the irreversible formation of a C=C bond, either in batch or in flow. Mechanistic studies support a canonical Mizoroki-Heck pathway where alkene insertion is the key step and multiple oxygen-atom coordination and Pd-iodine cluster flexibility allows to avoid intermolecular reactions. The significant advancement of this work is the use of relatively high concentrated reaction conditions for a metal-catalyzed macrocyclization reaction, which can now be run in flow. The results here presented open new avenues to the design of macrocyclization reactions under concentrated reaction conditions, with obvious operative, economic and environmental advantages.[27]

Experimental section

General procedures to prepare macrocycles. Two-step procedure

In a 2 mL glass vial equipped with a magnetic stir bar, 0.127 mmol of the corresponding o-iodoaryl cinnamate, 0.127 mL of NMP (1 M), 0.2 mmol of Na$_2$CO$_3$, 0.1 mmol of tetrapropylammonium bromide and palladium acetate (2 mol%) were added. The mixture was placed in a pre-heated oil bath and magnetically stirred at 140 °C. Aliquots (3 μL) were periodically taken out, diluted in a solution of the internal standard in dichloromethane, and analyzed by CG. After 3 h, the reaction mixture was cooled, 4 mL of water were added and the mixture was extracted with 3 mL ethyl acetate (three times), washed with brine and dried over magnesium sulfate. Products were purified by flash chromatography in a n-hexane: ethyl acetate (5:1) mixture as an eluent. *One-pot procedure: o*-Iodobenzyl bromide (53.4 μL, 0.45 mmol), DIPEA (149 μL, 0.9 mmol), and the corresponding ester (**6a–g** or **7a–b**, 0.3 mmol) were

Figure 6. Macrocyclization in flow with Pd$_{3\text{-}4}$/C as a solid catalyst. Reaction conditions: linear ω-iodide cinnamate **1a**, o-xylene (0.5 M), Cy$_2$NMe (1.5 equivalents); 0.1 mL h^{-1} of flow speed, 1 g of [Pd(NCs)/C (3.8 wt.% of Pd) pelletized with SiO$_2$ (50:50 in wt%)]. The pelletized material (0.2–0.4 μm) was introduced in a $^1/_4$ inch wide and 23 cm long tubular reactor. Error bars account for a 5% uncertainty.

ChemSusChem

Research Article
doi.org/10.1002/cssc.202300200

Chemistry Europe
European Chemical
Societies Publishing

charged in a reaction vessel under nitrogen. The mixture was heated at 150 °C (oil bath) for 2 h. After the starting material was completely consumed, 0.3 mL of NMP (1 M), 0.03 mmol of tetrapropylammonium bromide and palladium acetate (2 mol %) were added. After 3 h, the reaction mixture was cooled, 8 mL of water were added and the mixture was extracted with 6 mL ethyl acetate (three times), washed with brine and dried over magnesium sulfate. Products were purified as above.

Procedure for the macrocyclization reaction of 1 a with heterogeneous catalysts in batch

In a 2 mL glass vial equipped with a magnetic stir bar, 0.127 mmol of **1 a**, 0.127 mL of *o*-xylene (1 M), 0.2 mmol of Cy$_2$NMe and Pd$_{3-4}$/C (20 mol %) were added. The mixture was placed in a pre-heated oil bath and magnetically stirred at 100 °C. Aliquots (3 μL) were periodically taken out, diluted in a solution of the internal standard in dichloromethane, and analyzed by CG. After 20 h, the reaction mixture was cooled, 4 mL of water were added and the mixture was extracted with 3 mL ethyl acetate (three times), washed with brine and dried over magnesium sulfate, to give the desired macrocycle product **2 a**.

Conflict of Interests

The authors declare no conflict of interest.

Data Availability Statement

The data that support the findings of this study are available from the corresponding author upon reasonable request.

Keywords: macrocyclization · high concentration · Mizoroki-Heck reaction · Pd clusters · solid catalysts

[1] a) F. Davis, S. Higson, *Macrocycles: Construction, Chemistry and Nanotechnology Applications*, Wiley & Sons, **2011**; b) E. Marsault, M. L. Peterson, *Practical Medicinal Chemistry with Macrocycles: Design, Synthesis, and Studies*, Wiley & Sons, **2017**.

[2] a) T. O. Ronson, J. K. Richard, I. J. S. Fairlamb, *Tetrahedron* **2015**, *71*, 989–1009; b) C. Nájera, I. P. Beletskaya, M. Yus, *Chem. Soc. Rev.* **2019**, *48*, 4515–4618; c) D. G. Rivera, G. M. Ojeda–Carralero, L. Reguera, E. V. Van der Eycken, *Chem. Soc. Rev.* **2020**, *49*, 2039–2059; d) I. Saridakis, D. Kaiser, N. Maulide, *ACS Cent. Sci.* **2020**, *6*, 1869–1889; e) A. Furstner, *Acc. Chem. Res.* **2021**, *54*, 861–874.

[3] E. Marsault, M. L. Peterson, *J. Med. Chem.* **2011**, *54*, 1961–2004.

[4] a) Z. C. Girvin, M. K. Andrews, X. Liu, S. H. Gellman, *Science* **2019**, *366*, 1528–1531; b) L. Reguera, D. G. Rivera, *Chem. Rev.* **2019**, *119*, 9836–9860; c) S. Roesner, G. J. Saunders, I. Wilkening, E. Jayawant, J. V. Geden, P. Kerby, A. M. Dixon, R. Notman, M. Shipman, *Chem. Sci.* **2019**, *10*, 2465–2472; d) V. Adebomi, R. D. Cohen, R. Wills, H. A. H. Chavers, G. E. Martin, M. Raj, *Angew. Chem. Int. Ed.* **2019**, *58*, 19073–19080; e) D. Sindhikara, M. Wagner, P. Gkeka, S. Gussregen, G. Tiwari, G. Hessler, E. Yapici, Z. Li, A. Evers, *J. Med. Chem.* **2020**, *63*, 12100–12115; f) F. Esteve, B. Altava, M. Bolte, M. I. Burguete, E. Garcia–Verdugo, S. V. Luis, *J. Org. Chem.* **2020**, *85*, 1138–1145; g) D. B. Diaz, S. D. Appavoo, A. F. Bogdanchikova, Y. Lebedev, T. J. McTiernan, G. P. Gomes, A. K. Yudin, *Nat. Chem.* **2021**, *13*, 218–225.

[5] T. Newhouse, P. S. Baran, R. W. Hoffmann, *Chem. Soc. Rev.* **2009**, *38*, 3010–3021.

[6] a) C. Shu, X. Zeng, M–H. Hao, X. Wei, N. K. Yee, C. A. Busacca, Z. Han, V. Farina, C. H. Senanayake, *Org. Lett.* **2008**, *10*, 1303–1306; b) V. Farina, C. Shu, X. Zeng, X. Wei, Z. Han, N. K. Yee, C. H. Senanayake, *Org. Process Res. Dev.* **2009**, *13*, 250–254; c) X. Wei, C. Shu, N. Haddad, X. Zeng, N. D. Patel, Z. Tan, J. Liu, H. Lee, S. Shen, S. Campbell, R. J. Varsolona, C. A. Busacca, A. Hossain, N. K. Yee, C. H. Senanayake, *Org. Lett.* **2013**, *15*, 1016–1019; d) A. Sytniczuk, M. Dąbrowski, L. Banach, M. Urban, S. Czarnocka–Śniadała, M. Milewski, A. Kajetanowicz, K. Grela, *J. Am. Chem. Soc.* **2018**, *140*, 8895–8901; e) F. Ziegler, J. Teske, I. Elser, M. Dyballa, W. Frey, H. Kraus, N. Hansen, J. Rybka, U. Tallarek, M. R. Buchmeiser, *J. Am. Chem. Soc.* **2019**, *141*, 19014–19022.

[7] S. Beer, K. Brandhorst, J. Grunenberg, C. G. Hrib, P. G. Jones, M. Tamm, *Org. Lett.* **2008**, *10*, 981–984.

[8] a) G. Illuminati, L. Mandolini, *Acc. Chem. Res.* **1981**, *14*, 95–102; b) J. Blankenstein, J.–P. Zhu, *Eur. J. Org. Chem.* **2005**, 1949–1964; c) V. Martí–Centelles, M. D. Pandey, M. I. Burguete, S. V. Luis, *Chem. Rev.* **2015**, *115*, 8736–8834.

[9] T. Yuan, T. Ye, P. Zhao, S. Teng, Y. Yi, J. Wang, C. Shan, L. Wojtas, J. Jean, H. Chen, S. Xiadong, *Chem* **2020**, *6*, 1420–1431.

[10] A. R. Bogdan, K. James, *Chem. Eur. J.* **2010**, *16*, 14506.

[11] a) A. D. Curzons, D. J. C. Constable, D. N. Mortimer, V. L. Cunningham, *Green Chem.* **2001**, *3*, 1–6; b) D. J. C. Constable, A. D. Curzons, V. L. Cunningham, *Green Chem.* **2002**, *4*, 521–527; c) P. Anastas, N. Eghbali, *Chem. Soc. Rev.* **2010**, *39*, 301–312.

[12] a) K. Akaji, K. Teruya, M. Akaji, S. Aimoto, *Tetrahedron* **2001**, *57*, 2293–2303; b) X. Hemu, J. To, X. Zhang, J. P. Tam, *J. Org. Chem.* **2020**, *85*, 1504–1512.

[13] a) A. Leyva–Pérez, J. Oliver–Meseguer, P. Rubio–Marqués, A. Corma, *Angew. Chem. Int. Ed.* **2013**, *52*, 11554–11559; b) E. Fernández, M. A. Rivero-Crespo, I. Domínguez, P. Rubio–Marqués, J. Oliver-Meseguer, L. Liu, M. Cabrero-Antonino, R. Gavara, J. C. Hernandez–Garrido, M. Boronat, A. Leyva–Perez, A. Corma, *J. Am. Chem. Soc.* **2019**, *141*, 1928–1940.

[14] a) F. Garnes–Portolés, R. Greco, J. Oliver-Meseguer, J. Castellanos–Soriano, M. C. Jiménez, M. López-Haro, J. C. Hernández–Garrido, M. Boronat, R. Pérez–Ruiz, A. Leyva–Pérez, *Nat. Catal.* **2021**, *4*, 293–303; b) N. Jeddi, N. W. J. Scott, I. J. S. Fairlamb, *ACS Catal.* **2022**, *12*, 11615–11638.

[15] a) F. E. Ziegler, U. R. Chakraborty, R. B. Weisenfeld, *Tetrahedron* **1981**, *37*, 4035–4040; b) J. Jägel, M. E. Maier, *Synthesis* **2009**, *17*, 2881–2892; c) J. L. Carr, D. A. Offermann, M. D. Holdom, P. Dusart, A. J. P. White, A. J. Beavil, R. J. Leatherbarrow, S. D. Lindell, P. J. Sutton, A. C. Spivey, *Chem. Commun.* **2010**, *46*, 1824–1826; d) M. Groh, D. Meidlinger, G. Bringmann, A. Speicher, *Org. Lett.* **2012**, *14*, 4548–4551.

[16] a) J. K. Stille, M. Tanaka, *J. Am. Chem. Soc.* **1987**, *109*, 3785–3786; b) J. E. Baldwin, R. M. Adlington, S. H. Ramcharitar, *J. Chem. Soc. Chem. Commun.* **1991**, 940–942; c) A. Kalivretenos, J. K. Stille, L. S. Hegedus, *J. Org. Chem.* **1991**, *56*, 2883–2894; d) H. Fukuda, S. Nakamura, T. Eguchi, Y. Iwabuchi, N. Kanoh, *Synlett* **2010**, 2589–2592; e) W. P. Unsworth, K. A. Gallagher, M. Jean, J. P. Schmidt, L. J. Diorazio, R. J. K. Taylor, *Org. Lett.* **2012**, *15*, 262–265.

[17] a) N. Miyaura, H. Suginome, A. Suzuki, *Tetrahedron Lett.* **1984**, *25*, 761–764; b) P. J. Mohr, R. L. Halcomb, *J. Am. Chem. Soc.* **2003**, *125*, 1712–1713; c) G. A. Molander, F. Dehmel, *J. Am. Chem. Soc.* **2004**, *126*, 10313–10318; d) M. Dieckmann, M. Kretschmer, P. Li, S. Rudolph, D. Herkommer, D. Menche, *Angew. Chem. Int. Ed.* **2012**, *51*, 5667–5670; e) J. R. Cochrane, J. M. White, U. Wille, C. A. Hutton, *Org. Lett.* **2012**, *14*, 2402–2405.

[18] a) J. A. Porco, F. J. Schoenen, T. J. Stout, J. Clardy, S. L. Schreiber, *J. Am. Chem. Soc.* **1990**, *112*, 7410–7411; b) Y. Koyama, M. J. Lear, F. Yoshimura, I. Ohashi, T. Mashimo, M. Hirama, *Org. Lett.* **2005**, *7*, 267–270.

[19] a) B. M. Trost, S. J. Brickner, *J. Am. Chem. Soc.* **1983**, *105*, 568–575; b) T. Hu, E. J. Corey *Org. Lett.* **2002**, *4*, 2441–2443.

[20] a) X. Zhang, G. Lu, M. Sun, M. Mahankali, Y. Ma, M. Zhang, W. Hua, Y. Hu, Q. Wang, J. Chen, *Nat. Chem.* **2018**, *10*, 540–548; b) J. Tang, H. Chen, Y. He, W. Sheng, Q. Bai, H. Wang, *Nat. Commun.* **2018**, *9*, 1–8; c) B. Li, X. Li, B. Han, Z. Chen, X. Zhang, G. He, G. Chen, *J. Am. Chem. Soc.* **2019**, *141*, 9401–9407; d) J. Tan, J. Wu, S. Liu, H. Yao, H. Wang, *Sci. Adv.* **2019**, *5*, eaaw0323; e) Z. Bai, C. Cai, W. Sheng, Y. Ren, H. Wang, *Angew. Chem. Int. Ed.* **2020**, *59*, 14686–14692; f) X. Li, L. Qi, B. Li, Z. Zhao, G. He, G. Chen, *Org. Lett.* **2020**, *22*, 6209–6213; g) M.-M. Wang, S.-M. Lu, C. Li, *ACS Catal.* **2022**, *12*, 10801–10807.

[21] C. Nájera, *ChemCatChem* **2016**, *8*, 1865–1881.

[22] a) J. C. Collins, K. James, *MedChemComm* **2012**, *3*, 1489–1495; b) F. Garnes–Portolés, J. Sánchez–Quesada, E. Espinós–Ferri, A. Leyva–Pérez, *Synlett* **2022**, *33*, 1933–1937.

[23] a) L. Botella, C. Najera, *Angew. Chem. Int. Ed.* **2002**, *41*, 179–181; b) A. H. M. de Vries, J. M. C. A. Mulders, J. H. M. Mommers, H. J. W. Henderickx, J. G. de Vries, *Org. Lett.* **2003**, *5*, 3285–3288; c) J. G. De Vries, *Dalton Trans.* **2006**, *3*, 421–429; d) V. P. Ananikov, I. P. Beletskaya, *Organometallics* **2012**, *31*, 1595–1604.

[24] J. Campora, J. A. Lopez, P. Palma, P. Valerga, E. Spillner, E. Carmona, *Angew. Chem. Int. Ed.* **1999**, *38*, 147–151.

[25] a) G. Kundu, F. Opincal, T. Sperger, F. Schoenebeck, *Angew. Chem. Int. Ed.* **2022**, *61*, e202113667; b) M. Mendel, L. Gnägi, U. Dabranskaya, F. Schoenebeck, *Angew. Chem. Int. Ed.* **2022**, e202211167.

[26] a) J. Sa, A. Goguet, S. F. R. Taylor, R. Tiruvalam, C. J. Kiely, M. Nachtegaal, G. J. Hutchings, C. Hardacre, *Angew. Chem. Int. Ed.* **2011**, *50*, 8912–8916; b) J. Sa, S. F. R. Taylor, H. Daly, A. Goguet, R. Tiruvalam, Q. He, C. J. Kiely, G. J. Hutchings, C. Hardacre, *ACS Catal.* **2012**, *2*, 552–560; c) J. Oliver–Meseguer, I. Dominguez, R. Gavara, A. Doménech–Carbó, J. M. González–Calbet, A. Leyva–Pérez, A. Corma *Chem. Commun.* **2017**, *53*, 1116–1119.

[27] a) J. C. Collins, K. A. Farley, C. Limberakis, S. Liras, D. Price, K. James, *J. Org. Chem.* **2012**, *77*, 11079–11090; b) A.–C. Bedard, S. K. Collins, *Chem. Commun.* **2012**, *48*, 6420–6422; c) A.–C. Bedard, S. Regnier, S. K. Collins, *Green Chem.* **2013**, *15*, 1962–1966; d) R. D. Wills, V. T. Adebomi, M. Raj, *Synlett* **2020**, *31*, 1537–1542.